

Geometry-Aware Face Reconstruction Under Occluded Scenes

Dapeng Zhao^a

^aZhejiang Lab, Hangzhou, China

Abstract

Recently, deep learning-based 3D face reconstruction methods have demonstrated promising advancements in terms of quality and efficiency. Nevertheless, these techniques face challenges in effectively handling occluded scenes and fail to capture intricate geometric facial details. Inspired by the principles of GANs and bump mapping, we have successfully addressed these issues. Our approach aims to deliver comprehensive 3D facial reconstructions, even in the presence of occlusions. While maintaining the overall shape's robustness, we introduce a mid-level shape refinement to the fundamental structure. Furthermore, we illustrate how our method adeptly extends to generate plausible details for obscured facial regions. We offer numerous examples that showcase the effectiveness of our framework in producing realistic results, where traditional methods often struggle. To substantiate the superior adaptability of our approach, we have conducted extensive experiments in the context of general 3D face reconstruction tasks, serving as concrete evidence of its regulatory prowess compared to manual occlusion removal methods.

Keywords: 3D face reconstruction, Face alignment, Occluded scenes

1. Introduction

In the digital economy era, deriving a human face's shape from a single image is a cutting-edge area of research [Vetter and Blanz \(1998\)](#). As individuals seek an improved quality of life, the challenge of face recognition in obstructed settings has gained significant attention, closely tied to 3D face reconstruction. Yet, many recent reconstruction methods prioritize texture accuracy, often overlooking extreme scenarios. Thanks to advancements in deep learning, certain techniques can yield intricate 3D facial shapes [Richardson et al. \(2017\)](#); [Sela et al. \(2017\)](#). However, when faces are partially occluded, these methods tend to either reconstruct occlusions indiscriminately or fail outright. In the past, researchers commonly relied on shape-from-shading (SfS) methods [Kemelmacher-Shlizerman and Basri \(2010\)](#); [Li et al. \(2014\)](#) to capture geometric details.

In most cases, general face reconstruction methods often fail to provide geometric details [Guo et al. \(2020\)](#); [Hassner \(2013\)](#); [Taigman et al. \(2014\)](#); [Tuan Tran et al. \(2017\)](#) or typically provide few details [Hassner \(2013\)](#) to avoid reconstruction failures in extreme, challenging, unconstrained scenes. Most of these methods are based on localizing facial landmarks [Taigman et al. \(2014\)](#); [Jackson et al. \(2017\)](#); [Zhu et al. \(2016b\)](#). Unlike previous work, we describe an approach designed to attain both goals: Detailed 3D face reconstruction and robustness to occluded conditions.

The main contributions are summarized as follows:

- We propose an algorithm that combines facial landmarks and the face parsing map to identify the occluded region.
- To reconstruct the occluded area, we design a synthesis subnet that employs the predicted landmarks as guidance.
- We propose a novel 3D face reconstruction method that can produce reasonable face geometry details under occluded scenes.

Email address: mirror1775@gmail.com (Dapeng Zhao)

2. RELATED ARTS

2.1. 3D Morphable Model

With the advancement of deep learning, significant progress has been made in 3D reconstruction, especially in the context of face reconstruction, utilizing Convolutional Neural Networks. The method proposed by Anh *et al.* Tuan Tran *et al.* (2017) offers both dense face alignment and facial model results. However, the effectiveness of these approaches is constrained by the limitations inherent in the 3D space defined by templates.

In contrast, some recent end-to-end techniques Jackson *et al.* (2017); Feng *et al.* (2018) have achieved state-of-the-art performance in their respective domains. These methods, however, typically directly reconstruct the facial model without the need for input image identification or processing. VRN Jackson *et al.* (2017) introduces an innovative deep 3D face reconstruction approach that eliminates the necessity for precise alignment and the establishment of dense image correspondences, requiring only a single 2D facial image. VRN significantly widens the range of applications for 3D face technology. On the other hand, PRNet Feng *et al.* (2018) has devised a straightforward method for simultaneously reconstructing the 3D facial structure. This approach incorporates a UV position map to record the 3D facial shape in UV space.

2.2. Generative Adversarial Nets

Under normal circumstances, we believe that Generative Adversarial Nets (GANs) are among the few tools capable of achieving a reconstruction effect in the 2D face field. After identifying and removing the occluded areas, we employ GAN to synthesize the facial image while preserving a reasonable topological structure. GAN typically comprises a generator and a discriminator, which engage in a competitive process. In the realm of 2D images, GAN stands out as one of the most effective tools for face synthesis. GAN has found successful applications in the fields of image manipulation Abdal *et al.* (2019); Jaderberg *et al.* (2015); Lee *et al.* (2020); Zhu *et al.* (2016a) and image-to-image translation Isola *et al.* (2017); Park *et al.* (2019); Liu *et al.* (2017); Wang *et al.* (2018); Zhu *et al.* (2017).

2.3. Facial Landmark Detection

Traditional facial landmark detectors are more regression-based. Valstar *et al.* Valstar *et al.* (2010) predict landmark locations from face image patches using support vector regression (SVR). Cao *et al.* Cao *et al.* (2014) use cascaded regression with pixel-difference features. Several other works Cootes *et al.* (2012); Dantone *et al.* (2012); Yang and Patras (2013) employ random regression forests to cast votes for landmark locations based on local face images. In these methods, an initial landmark position is first randomly selected, and then the facial landmarks are iteratively predicted. Therefore, the quality of the initial position is crucial.

3. Our Method

As shown in Figure 1, our method is divided into two phases: the final output of stage 1 is to remove the 2D face picture of the occlusion; the final output of stage 2 is a 3D face model with geometric details.

3.1. Landmark Prediction Network

Face alignment (especially accurate facial landmark $\mathbf{L}_{\text{face}} \in \mathbb{R}^{2 \times 68}$ generation) is the basis of the whole framework (Section 1 of Figure 1). The closest approach to our method is MobileNet-V3 model Howard *et al.* (2019). The network \mathcal{N}_{pre} aims to generate \mathbf{L}_{face} from a face image \mathbf{I}_0 : $\mathbf{L}_{\text{face}} = \mathcal{N}_L(\mathbf{I}_0; \theta_{land})$, where θ_{land} denotes the parameters to be trained. Since our task is to export face features rather than identify different people, we design the loss function as follows:

$$\mathcal{L}_{lmk} = \|\mathbf{L}_{\text{face}} - \mathbf{L}_{\text{gt}}\|_2^2 \quad (1)$$

where \mathbf{L}_{gt} is the ground truth face landmarks and $\|\cdot\|_2$ is the L_2 norm.

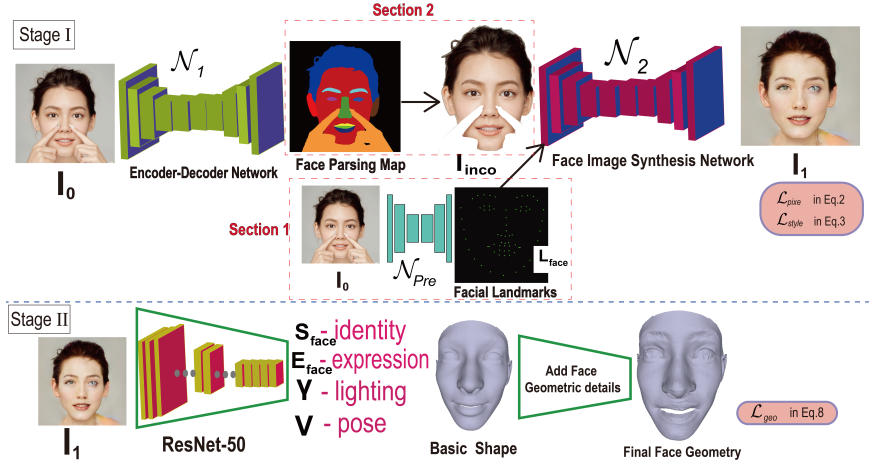


Figure 1: Our method overview.

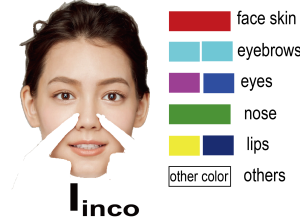


Figure 2: Face parsing network of our method.

3.2. Face Synthesis Network

Overall, We design the image synthesis module \mathcal{N}_s to synthesize a 2D face that removes the occlusion region. The module includes three parts: matting operator (Section 2 of Figure 1), generator and discriminator.

Matting operator. Typically, the task of the Matting operator \mathcal{N}_1 is to remove the occluded areas \mathbf{I}_m of the input photo \mathbf{I}_0 (Figure 2). For each input face image $\mathbf{I}_{in} \in \mathbb{R}^{H \times W \times 3}$, we utilized the trained model \mathcal{N}_1 to estimate pixel-level label classes and generate the face parsing map $\mathbf{Q} \in \mathbb{R}^{H \times W \times 1}$. According to the map \mathbf{Q} , we identify and remove the occluded area \mathbf{I}_m to obtain the hollowed-out photo \mathbf{I}_{inco} . This will be the input for our next task.

Generator. The generator \mathcal{N}_2 desires to generate the complete face by taking hollowed-out images \mathbf{I}_{inco} and landmarks \mathbf{L} (\mathbf{L}_{face} or \mathbf{L}_{gt}). More specifically, the network includes gradually down-sampled encoding blocks. These blocks are composed of subordinate residual blocks with dilated convolutions and an attention block. The generator can be formulated as $\mathbf{I}_1 = \mathcal{N}_2(\mathbf{I}_{inco}, \mathbf{L}; \theta_2)$, with θ_2 the trainable parameters.

Discriminator. The purpose of the discriminator is to judge whether the data distribution meets our requirements. The ambition of face synthesis is achieved when the generated results are not distinguishable from the real ones.

Loss Function. We use a combination of per-pixel loss and style loss for training the face synthesis network. We compute the per-pixel loss as follows:

$$\mathcal{L}_{pixe} = \frac{1}{M_s} \|\mathbf{I}_1 - \mathbf{I}_0\| \quad (2)$$

where M_s denotes the mask size and $\|\cdot\|$ stands for the L_1 norm. Notice that we use M_s as the denominator and its role is to adjust the penalty.

The style loss computes the style distance between two images as follows:

$$\mathcal{L}_{style} = \sum_n \frac{1}{R_n \times R_n} \left\| \frac{B_n(\mathbf{I}_1 \odot \mathbf{I}_m) - G_n(\mathbf{I}_0 \odot \mathbf{I}_m)}{R_n \times H_n \times W_n} \right\| \quad (3)$$

where $B_n(x) = \varphi_n(x)^T \varphi_n(x)$ denotes the Gram Matrix corresponding to $\varphi_n(x)$, $\varphi_n(\cdot)$ stands for the R_n feature maps with the size $H_n \times W_n$ of the n -th layer.

The total loss with respect to the face synthesis module:

$$\mathcal{L}_{final} = \lambda_{pixe} \mathcal{L}_{pixe} + \lambda_{style} \mathcal{L}_{style} \quad (4)$$

here, we use $\lambda_{pixe} = 1$, $\lambda_{style} = 250$ in our experiments.

3.3. Construct the Fundamental Shapes

We utilize the hot deep learning method in recent years to regress the 3DMM coefficients to construct the basic face shape. The primary face model is formulated as follows:

$$\mathbf{S}_{face} = \bar{\mathbf{S}} + \sum_{i=1}^{m-1} \alpha_i \mathbf{s}_i \quad (5)$$

where $\bar{\mathbf{S}}$ denotes an average 3D face shape, m denotes the number of faces participating in the weighted face datasets, \mathbf{s}_i denotes the i th face shape and α_i denotes the face shape coefficients estimated from \mathbf{I}_1 .

Similarly, we model the expressions using the following formulation:

$$\mathbf{E}_{face} = \sum_{j=1}^{m-1} \beta_j \mathbf{e}_j \quad (6)$$

where β_j denotes the expression coefficients and \mathbf{e}_j denotes the j th expression.

Further, we denote the viewpoint as $\mathbf{v} = [\mathbf{r}^T, \mathbf{t}^T]$, where $\mathbf{r} \in \mathbb{R}^3$ denotes the 3D rotation, expressed by Euler angles, and $\mathbf{t} \in \mathbb{R}^3$ denotes a translation vector, together aligning a generic 3D face shape with the face appearing in \mathbf{I}_1 .

We adopt the Basel Face Model (BFM) Paysan et al. (2009), which provides both $\bar{\mathbf{S}}$, \mathbf{s}_i and \mathbf{e}_i . We approximated the scene illumination with Spherical Harmonics (SH) Tewari et al. (2020); Deng et al. (2020, 2019) parameterized by coefficient vector $\gamma \in \mathbb{R}^9$. Given \mathbf{I}_1 , we estimate $y = (\mathbf{S}_{face}, \mathbf{E}_{face}, \mathbf{V}, \gamma)$ using the recent deep 3DMM approach of Yu et al. Deng et al. (2019), with their pre-trained model.

3.4. Recovering Face Geometric Details

Inspired by the method of image-to-image translation Isola et al. (2017); n et al. (2018), we define the displacements of the depth map as the distances through the pixels of \mathbf{I}_1 to the 3D face surface. Generally, we define the bump map $\Phi(\mathbf{b})$ as:

$$\Phi(\mathbf{b}) = \begin{cases} \phi(0) & \text{other} \\ \phi(d'(\mathbf{b}) - d(\mathbf{b})) & \text{face projects to } \mathbf{b} \end{cases} \quad (7)$$

where $\phi(\cdot)$ denotes an encoding function that converts the depth value to the linear range $[0, \dots, 255]$, \mathbf{b} denotes the pixel coordinate $[x, y]$ in \mathbf{I}_1 , $d'(\mathbf{b})$ denotes the depth, which is the distance from the surface of the detailed face shape to \mathbf{b} along the line of sight, $d(\mathbf{b})$ denotes the depth of the basic shape.

Thus, Given a bump map Φ and the depth of the basic shape, we can compute the detailed depth follows $d'(\mathbf{b}) = d(\mathbf{b}) + \phi^{-1}(\Phi(\mathbf{b}))$.

In order to increase geometric details and to suppress noise, we define the loss function as follows:

$$\mathcal{L}_{geo} = \left\| \tilde{\Phi} - \Phi \right\| + \left\| \frac{\partial \tilde{\Phi}}{\partial x} - \frac{\partial \Phi}{\partial x} \right\| + \left\| \frac{\partial \tilde{\Phi}}{\partial y} - \frac{\partial \Phi}{\partial y} \right\| \quad (8)$$

where $\|\cdot\|$ denotes the L_1 norm, $\tilde{\Phi}$ denotes the ground truth and $\frac{\partial\tilde{\Phi}}{\partial x}, \frac{\partial\tilde{\Phi}}{\partial y}$ denotes the 2D gradient of the bump map. We found that by adding these last two terms of loss function and we reduce bump map noise by favoring smoother surfaces. At the same time, the final effect shows that high-frequency details are preserved.

4. Experimental results



Figure 3: Comparison of qualitative results. Baseline methods from left to right: Sela *et al.*, PRNet, 3DDFA, and our method.

Figure 3 shows our reconstruction results compared with the contemporary arts Sela *et al.* (2017); Guo *et al.* (2020); Feng *et al.* (2020). It can be clearly seen from the Figure 3 that Sela *et al.*'s method shows the shape of various obstructions. This may be due to the method focusing too much on the local shape (Figure 4). Since the other two methods are based on existing 3D face model templates, the shapes are too smooth and lack geometric details.

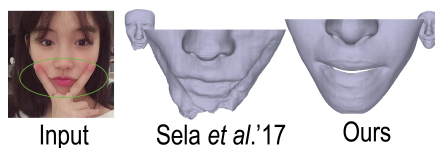


Figure 4: Comparison of local facial geometric details.

5. Conclusions

We describe an approach capable of producing detailed 3D face reconstructions from images taken in occluded conditions. The advantage of our method is that it can effectively process the facial details in places where the face is occluded. Since the previous arts are limited to the reconstruction of faces in non-occluded scenes, our method represents a leap in 3D facial details reconstruction capabilities. Unlike the recently popular end-to-end reconstruction method, our method is a two-stage face reconstruction task based on basic shapes.

References

- Abdal, R., Qin, Y., Wonka, P., 2019. Image2stylegan: How to embed images into the stylegan latent space?, in: Proceedings of the IEEE/CVF International Conference on Computer Vision, pp. 4432–4441.
- Cao, X., Wei, Y., Wen, F., Sun, J., 2014. Face alignment by explicit shape regression. *International Journal of Computer Vision* 107, 177–190.
- Cootes, T.F., Ionita, M.C., Lindner, C., Sauer, P., 2012. Robust and accurate shape model fitting using random forest regression voting, in: *European Conference on Computer Vision*, Springer. pp. 278–291.
- Dantone, M., Gall, J., Fanelli, G., Van Gool, L., 2012. Real-time facial feature detection using conditional regression forests, in: 2012 IEEE Conference on Computer Vision and Pattern Recognition, IEEE. pp. 2578–2585.
- Deng, Y., Yang, J., Chen, D., Wen, F., Tong, X., 2020. Disentangled and controllable face image generation via 3d imitative-contrastive learning, in: *Proceedings of the IEEE/CVF Conference on Computer Vision and Pattern Recognition*, pp. 5154–5163.
- Deng, Y., Yang, J., Xu, S., Chen, D., Jia, Y., Tong, X., 2019. Accurate 3d face reconstruction with weakly-supervised learning: From single image to image set, in: *Proceedings of the IEEE Conference on Computer Vision and Pattern Recognition Workshops*, pp. 0–0.
- Feng, Y., Feng, H., Black, M.J., Bolkart, T., 2020. Learning an animatable detailed 3d face model from in-the-wild images. *ACM Transactions on Graphics (TOG)* 40, 1–13.
- Feng, Y., Wu, F., Shao, X., Wang, Y., Zhou, X., 2018. Joint 3d face reconstruction and dense alignment with position map regression network, in: *Proceedings of the European Conference on Computer Vision (ECCV)*, pp. 534–551.
- Guo, J., Zhu, X., Yang, Y., Yang, F., Lei, Z., Li, S.Z., 2020. Towards fast, accurate and stable 3d dense face alignment. *arXiv preprint arXiv:2009.09960* .
- Hassner, T., 2013. Viewing real-world faces in 3d, in: *Proceedings of the IEEE International Conference on Computer Vision*, pp. 3607–3614.
- Howard, A., Sandler, M., Chu, G., Chen, L.C., Chen, B., Tan, M., Wang, W., Zhu, Y., Pang, R., Vasudevan, V., 2019. Searching for mobilenetv3, in: *Proceedings of the IEEE/CVF International Conference on Computer Vision*, pp. 1314–1324.
- Isola, P., Zhu, J.Y., Zhou, T., Efros, A.A., 2017. Image-to-image translation with conditional adversarial networks, in: *Proceedings of the IEEE conference on computer vision and pattern recognition*, pp. 1125–1134.
- Jackson, A.S., Bulat, A., Argyriou, V., Tzimiropoulos, G., 2017. Large pose 3d face reconstruction from a single image via direct volumetric cnn regression, in: *Proceedings of the IEEE International Conference on Computer Vision*, pp. 1031–1039.
- Jaderberg, M., Simonyan, K., Zisserman, A., Kavukcuoglu, K., 2015. Spatial transformer networks. *arXiv preprint arXiv:1506.02025* .
- Kemelmacher-Shlizerman, I., Basri, R., 2010. 3d face reconstruction from a single image using a single reference face shape. *IEEE transactions on pattern analysis and machine intelligence* 33, 394–405.
- Lee, C.H., Liu, Z., Wu, L., Luo, P., 2020. Maskgan: Towards diverse and interactive facial image manipulation, in: *Proceedings of the IEEE/CVF Conference on Computer Vision and Pattern Recognition*, pp. 5549–5558.
- Li, C., Zhou, K., Lin, S., 2014. Intrinsic face image decomposition with human face priors, in: *European conference on computer vision*, Springer. pp. 218–233.
- Liu, M.Y., Breuel, T., Kautz, J., 2017. Unsupervised image-to-image translation networks. *arXiv preprint arXiv:1703.00848* .
- Liu, M.Y., Hassner, T., Masi, I., Paz, E., Nirkin, Y., Medioni, G., 2018. Extreme 3d face reconstruction: Seeing through occlusions, in: *Proceedings of the IEEE Conference on Computer Vision and Pattern Recognition*, pp. 3935–3944.
- Park, T., Liu, M.Y., Wang, T.C., Zhu, J.Y., 2019. Semantic image synthesis with spatially-adaptive normalization, in: *Proceedings of the IEEE Conference on Computer Vision and Pattern Recognition*, pp. 2337–2346.
- Paysan, P., Knothe, R., Amberg, B., Romdhani, S., Vetter, T., 2009. A 3d face model for pose and illumination invariant face recognition, in: 2009 Sixth IEEE International Conference on Advanced Video and Signal Based Surveillance, Ieee. pp. 296–301.
- Richardson, E., Sela, M., Or-El, R., Kimmel, R., 2017. Learning detailed face reconstruction from a single image, in: *Proceedings of the IEEE Conference on Computer Vision and Pattern Recognition*, pp. 1259–1268.
- Sela, M., Richardson, E., Kimmel, R., 2017. Unrestricted facial geometry reconstruction using image-to-image translation, in: *Proceedings of the IEEE International Conference on Computer Vision*, pp. 1576–1585.
- Taigman, Y., Yang, M., Ranzato, M., Wolf, L., 2014. Deepface: Closing the gap to human-level performance in face verification, in: *Proceedings of the IEEE conference on computer vision and pattern recognition*, pp. 1701–1708.
- Tewari, A., Seidel, H.P., Elgharib, M., Theobalt, C., 2020. Learning complete 3d morphable face models from images and videos. *arXiv preprint arXiv:2010.01679* .
- Tuan Tran, A., Hassner, T., Masi, I., Medioni, G., 2017. Regressing robust and discriminative 3d morphable models with a very deep neural network, in: *Proceedings of the IEEE Conference on Computer Vision and Pattern Recognition*, pp. 5163–5172.
- Valstar, M., Martinez, B., Binefa, X., Pantic, M., 2010. Facial point detection using boosted regression and graph models, in: 2010 IEEE Computer Society Conference on Computer Vision and Pattern Recognition, IEEE. pp. 2729–2736.
- Vetter, T., Blanz, V., 1998. Estimating coloured 3d face models from single images: An example based approach, in: *European conference on computer vision*, Springer. pp. 499–513.
- Wang, T.C., Liu, M.Y., Zhu, J.Y., Tao, A., Kautz, J., Catanzaro, B., 2018. High-resolution image synthesis and semantic manipulation with conditional gans, in: *Proceedings of the IEEE conference on computer vision and pattern recognition*, pp. 8798–8807.
- Yang, H., Patras, I., 2013. Sieving regression forest votes for facial feature detection in the wild, in: *Proceedings of the IEEE International Conference on Computer Vision*, pp. 1936–1943.

- Zhu, J.Y., Krähenbühl, P., Shechtman, E., Efros, A.A., 2016a. Generative visual manipulation on the natural image manifold, in: European conference on computer vision, Springer. pp. 597–613.
- Zhu, J.Y., Park, T., Isola, P., Efros, A.A., 2017. Unpaired image-to-image translation using cycle-consistent adversarial networks, in: Proceedings of the IEEE international conference on computer vision, pp. 2223–2232.
- Zhu, X., Lei, Z., Liu, X., Shi, H., Li, S.Z., 2016b. Face alignment across large poses: A 3d solution, in: Proceedings of the IEEE conference on computer vision and pattern recognition, pp. 146–155.